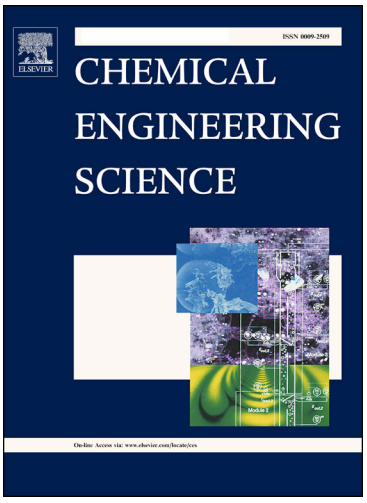

Transesterification of Soybean and Castor Oil with methanol and butanol Using Heterogeneous Basic Catalysts to obtain Biodiesel

Marisa B. Navas, Patricia A. Bolla, Ileana D. Lick, Mónica L. Casella, José F. Ruggera

PII: S0009-2509(18)30282-3
DOI: https://doi.org/10.1016/j.ces.2018.04.068
Reference: CES 14200

To appear in: *Chemical Engineering Science*

Received Date: 9 November 2017
Revised Date: 13 April 2018
Accepted Date: 28 April 2018

Please cite this article as: M.B. Navas, P.A. Bolla, I.D. Lick, M.L. Casella, J.F. Ruggera, Transesterification of Soybean and Castor Oil with methanol and butanol Using Heterogeneous Basic Catalysts to obtain Biodiesel, *Chemical Engineering Science* (2018), doi: https://doi.org/10.1016/j.ces.2018.04.068

Transesterification of Soybean and Castor Oil with methanol and butanol Using Heterogeneous Basic Catalysts to obtain Biodiesel

Marisa B. Navas[1], Patricia A. Bolla[1], Ileana D. Lick[1], Mónica L. Casella[1], José F. Ruggera[1*]

[1] *CINDECA, CCT-CONICET and Universidad Nacional de La Plata, calle 47 Nº 257 (1900) La Plata (Argentina)*

(*) corresponding author: jfruggera@quimica.unlp.edu.ar

Abstract

This paper focuses on the preparation and characterization of CaO, MgO and ZnO, both bulk and supported on γ-Al_2O_3 and their catalytic activity in the transesterification of soybean oil and castor oil with methanol and butanol in order to produce biodiesel. XRD, SEM, CO_2-adsorption followed by TGA and N_2 adsorption have been employed to characterize the prepared catalysts. In supported catalysts, the presence of γ-Al_2O_3 improves alcohol dissociation on the superficial basic sites. The first step of the reaction mechanism is then favored (hydrogen abstraction). In the transesterification of castor oil with butanol, MgO/ γ -Al_2O_3 and ZnO/ γ -Al_2O_3 catalysts showed high yields to FABE (Fatty Acid Butyl Ester) (97% and 85%, respectively). These last catalysts constitute an efficient alternative for obtaining second-generation biodiesel, taking into account that castor oil is a nonedible source and butanol is an alcohol that can be obtained from biomass.

Keywords: Biodiesel, Heterogeneous catalysts; Soybean oil; Castor oil; Transesterification; Mixed metal oxide

1. Introduction

Given the problems associated with climate change, the continued increase in the prices of oil and its derivatives, as well as a growing concern to ensure the supply of primary energy sources like oil, there is currently a great interest in the use of biomass–and particularly biofuels–for energy. Biofuels are a direct and immediate substitute for liquid fuels employed in the transportation area and can be easily integrated to the logistic systems currently in operation.

Among these liquid biofuels is biodiesel that is defined, according to ASTM 6751, as a mixture of monoalkyl esters of long-chain fatty acids derived from renewable lipids, which can be used in compression ignition engines. Its use as a fuel is possible due to certain characteristics of biodiesel: an appropriate viscosity, a high flash point, high cetane number, etc. (Nascimento *et al*.,2008). Biodiesel is also attractive from an environmental point of view: it comes from renewable sources, it is burned without a net contribution of CO_2 to the atmosphere and it does not contribute to the production of SOx (Lapuerta *et al.*, 2008; Prince *et al.*, 2008).

The commercially used method for the production of biodiesel is transesterification (Scheme 1). In this reaction, triglycerides react with low molecular weight alcohols to produce esters and glycerol. Glycerol is a by-product that can be used in cosmetics, food, etc. (Zeng et al., 2008). Typically, the transesterification reaction is carried out under homogeneous catalysis, using basic catalysts such as NaOH or KOH (Dias *et al*., 2008; Georgogianni *et al.*, 2009). The reaction occurs much faster with basic catalysts than with acid catalysts but has the disadvantage of forming unwanted by-products and soaps if the mixture contains free fatty acids, thus requiring an expensive separation process and using great amounts of water (Komers *et al.*, 2001).

The use of heterogeneous catalysts may be an acceptable solution. Some studies have found promising solid catalysts containing alkali and alkaline earth oxides such as CaO, BaO or SrO (Liu *et al.,* 2007; Patil *et al.*, 2009), and even salts supported on different metal oxides: KOH/Al_2O_3 (Noiroj *et al.,* 2009),

KF/MgO (Wan *et al.*, 2008), and calcined Mg-Al hydrotalcites (Brito *et al*., 2009). Pure MgO was also tested, presenting weak catalyst activity, owing to a weak basic strength and high solubility in methanol (Sharma *et al.*, 2011). Due to these drawbacks, several studies have focused on improving the acid-base characteristics of MgO. An alternative is to add other species like oxides, metal ions and noble metals (Lee *et al.,* 2013). On the other hand, ZnO is anamphoteric oxide, which possesses acid and basic sites, suitable for the transesterification of vegetable oils with high content of free fatty acids (FFA) (Yan *et al.*, 2009).

The use of vegetable oils as a source for the production of biodiesel has the advantage of their renewability, biodegradability, and lower contents of aromatic compounds and sulfides (Koh and Mohd-Ghazi, 2011). Vegetable oils used in the production of biodiesel depend mainly on the climate of each region, for example, soybean, canola or sunflower oils are usually used in Argentina, Brazil, the United States or Germany, while in India, biodiesel is produced from nonedible Jatropha oil (Ullah *et al.*, 2016). Research is focused on finding renewable sources that do not compete with the food industry to produce second-generation biodiesel.

With respect to the alcohols used in the transesterification reaction, the ones most often used are methanol, ethanol, propanol, butanol and amyl alcohol, the first two being the most frequently employed (Demirbas, 2003). Methanol is the least expensive of them and has certain physicochemical advantages, such as its polarity, but has the disadvantage of coming from the fossil fuel industry. In that sense, ethanol would be preferred, since it derives from agricultural products. It is also renewable and less environmentally harmful. Moreover, biobutanol (obtained from renewable sources) is a molecule that contains more energy than ethanol, but with the disadvantage of being more toxic. However, nowadays, butanol is considered a better alternative than ethanol as a biofuel since it is less corrosive and less soluble in water, therefore being a more suitable fuel for the internal combustion engines currently used in automobiles (Steen *et al.*, 2008).

As a contribution, this work presents the preparation and characterization of CaO, MgO and ZnO, both bulk and supported on γ-Al_2O_3. The catalytic activity was evaluated in the transesterification reaction between a vegetable oil and an alcohol. Soybean and castor oil, and methanol and butanol were chosen for the experimental work.

2. Experimental

2.1. Catalyst preparation

Mass and supported Ca, Mg and Zn oxides were prepared by the precipitation method. Typically, $Ca(NO_3)_2.4H_2O$ (Anedra, 99.1%), $Mg(NO_3)_2.6H_2O$ (Biopack, 98.0%) or $Zn(NO_3)_2.6H_2O$ (Anedra, 99.5%) were dissolved in distilled water, or in an aqueous suspension of γ-Al_2O_3, and stirred vigorously. The metal content was 0.27 mol%. Then, an aqueous solution of $(NH_4)_2CO_3$ (Anedra, 21.4%) 1M was added slowly to precipitate metal ions. The pH was regulated using an aqueous solution of NH_4OH (Anedra, 28.6%). For the preparation of Ca and Zn containing catalysts the pH was regulated between 7 and 8 and for Mg containing catalysts was regulated between 9 and 10. The solution was maintained under stirring for 2h, and then aged for a week. The precipitate was then filtered and dried at 60 °C overnight. Finally, the solid was calcined at the required temperature to obtain the oxide (Ngamcharussrivichai *et al.,* 2008; Teo *et al.*, 2014). The calcination temperatures for the different catalysts were determined from de thermal decomposition analysis.

2.2. Catalyst Characterization

The temperature of calcination to obtain the different oxides was selected by thermogravimetric analysis, using a Shimadzu TGA-50 analyzer. Samples were thermally treated in a 100 ml min^{-1} He flow. The variation of sample weight was determined from RT up to 800°C. From the mass loss information as a function of time, the derivative curve (DTGA) was obtained. The theoretical mass loss was calculated from Equation 1 (M: Ca, Mg or Zn), taking into account the decomposition of carbonates:

$$\%\ \text{theoretical mass loss} = \frac{MW\ CO_2}{MW\ MCO_3}\ X\ 100 \qquad (1)$$

where MW CO_2 and MW MCO_3 are the molecular weight of CO_2 and of the metal carbonate, respectively.

The total surface area was obtained by the Brunauer-Emmer-Teller (BET) method, using N_2 physisorption at 77 K, with a Micromeritics ASAP 2020 analyzer.

The basicity of the alumina and catalysts was estimated by thermogravimetric tests of CO_2 adsorption (Zhang *et al.*, 2014) using a Shimadzu TGA-50 equipment. Typically, around of 30 mg of sample was initially submitted to a heating ramp of 20 °C min^{-1} from RT up to 120 °C, in a He flow of 50 mL min^{-1}. The temperature was maintained at 120 °C for 30 min to remove adsorbed water and other volatiles. Then, the sample was cooled in a He flow to 75°C. At that temperature, the catalyst was exposed to an CO_2–He mixture (50 vol.%) at 100 mL min^{-1} flow for the adsorption, recording the increase of mass of the sample until a constant mass was obtained (15 min).

The surface morphology was determined using scanning electron microscopy (SEM), with a Philips SEM 505. X-ray diffraction was conducted using Cu Kα (λ=0.154 nm) as a radiation source in an automatic X-ray diffractometer Philips PW 1740. The samples were scanned from 5° to 75° at the scanning speed of 1 min^{-1}. The crystallite size was calculated using Debye-Scherrer's equation and the Williamson-Hall's method, which includes not only the contribution of the crystalline domain but also the microstrains (Equation 2).

$$\beta \cos\theta = \frac{k\lambda}{D} + 4\varepsilon \sin\theta \qquad (2)$$

where β is the ratio area/intensity, θ is the diffraction angle for each peak, κ a constant, λ the X-ray wavelength of radiation for CuKα, D is the crystallite size, and ε an equation to consider microstrains (β/4tgθ) (Patterson, 1939; Williamson and Hall, 1953).

2.3. Transesterification procedure

The catalytic activity was evaluated using soybean oil and castor oil (supplied by Union Química Argentina and Cicarelli, respectively), and methanol or butanol. The composition of vegetable oils is presented in Table 1.

Reactions were carried out in a 250 cm^3 three-necked batch reactor, equipped with a reflux condenser and a mechanical stirrer. Transesterification was performed under the following conditions: catalyst amount, 5 wt%; alcohol/oil ratio, 6:1; reaction time, 6 h; and reaction temperature, 60 °C for methanol and 80 °C for butanol.

Samples were analyzed by gas chromatography with a GC-2010 Plus Tracera, equipped with a BID detector and a capillary column (MEGA-Biodiesel 105, 15 m x 0.32 mm x 0.10 µm). The product analysis was performed according to EN 14105 and ASTM D6584 test methods. A temperature program was set, starting at 50 °C, followed by a ramp rate of 15 °C min^{-1} to 180 °C, then a ramp rate of 7 °C min^{-1} to 230 °C, and finally a ramp rate of 30 °C min^{-1} to 350 °C. The injector and detector temperatures were both 350 °C. The sample volume injected was 1 µL, with helium as the carrier gas, at a flow of 3 mL min^{-1}. Samples were taken at 2, 4 and 6 h. Then, 80 µL of (S)-(-)-1,2,4-butanetriol stock solution, 100 µL of tricaprin stock solution, and 100 µL of N-methyl-N-(trimethylsilyl)trifluoroacetamide (MSTFA) were added to 100 mg of the sample. The mixture was shaken for 20 min at room temperature, and finally 8 mL of n-heptane was added.

Conversion (X%) was calculated from Equation 3:

$$X\% = 100 * \left(1 - \frac{\left(\frac{At}{Astdt}\right)}{\left(\frac{A0}{Astd0}\right)}\right) \qquad (3)$$

where A_t is the triglycerides peaks area at time t (in hours), A_{stdt} is the tricaprin peak area at time t, A_0 is the triglycerides peaks area at zero hours, and A_{std0} is the tricaprin peak area at zero hours of reaction. Selectivity (S_i) to monoglycerides or diglycerides (S_m or S_d, respectively) is defined as follows (Equation 4):

$$S_i = 100 * \frac{1}{Fx} \left(\frac{\frac{Ax6}{Astd6}}{\frac{At0}{Astd0} - \frac{At6}{Astd6}} \right) \qquad (4)$$

where Fx is the response factor for monoglycerides or diglycerides; Ax_6 is the peak area for monoglycerides, diglycerides, at 6h of reaction, $Astd_6$ is the peak area of tricaprin at 6h of reaction; At_0 is the peak area at zero hours for triglycerides; At_6 is the peak area at 6 h for triglycerides and $Astd_0$ is the peak area of tricaprin at zero hours of reaction. FAME or FABE selectivity (S_{FAME} or S_{FABE}, respectively) was calculated with Equation 5.

$$S_{FAME/FABE} = 100 - S_m - S_d \qquad (5)$$

Finally, FAME or FABE yield was calculated as the product of selectivity to FAME or FABE and conversion.

2.4. Catalysts Leaching

For each catalytic test, after 6h, the reaction mixture was collected. The catalyst was removed after decantation and washed with dichloromethane to eliminate any oil residue adhered to the catalyst surface. The washed sample was then centrifuged and dried at room temperature. The metal content before and after reaction was analyzed by atomic absorption spectroscopy. For each test, the sample was treated with HNO_3 1:1 in a hot sand bath until complete digestion. Then, the necessary dilutions were prepared with deionized water. For every analysis, a 0.7 nm slit was used. The lines employed were 285.2 nm and 213.9 nm for Mg and Zn lamps, respectively.

3. Results and discussion

3.1 Morphological and textural properties

In order to study the decomposition of the Ca, Mg and Zn carbonates, thermogravimetric experiments were carried out. The thermograms obtained for mass precursors are shown in Figure 1; the weight loss can be observed as a function of temperature. In addition, the derivative of the weight loss curve, which indicates the rate of thermo-gravimetric phenomena, is presented in the secondary axis. When subject to a thermal treatment, carbonates are decomposed as follows (Scheme 2):

The weight loss can be attributed, at temperatures less than 100 °C, to the desorption of adsorbed water; and at higher temperatures, to the formation of CO_2. Table 2 shows the comparison between theoretical and experimental values of weight loss, in the temperature range 100 °C -750 °C. The percentages for weight loss obtained in the studied temperature range are similar to the theoretical ones (±3%), except in the case of $MgCO_3$. For this last sample, the weight loss was higher than expected, probably due to higher water content. The crystalline network of an alkaline earth oxide is more stable than that of a carbonate, therefore the decomposition of carbonates is favored. The alkaline earth carbonates thermal stability depends on the ionic potential of the metal, which is proportional to the charge and inversely proportional to the radius. The ionic radii of the Mg^{2+}, Zn^{2+} and Ca^{2+} species, in an octahedral environment, are 0.71, 0.88 and 1.14 Å respectively. Therefore, among the carbonates studied in this work, $CaCO_3$ is the most stable due to its greater radius. The different stability of magnesium carbonate and zinc carbonate, whose cations present similar ion radii, is due to the lower effective nuclear charge of Zn^{2+}, which is a transition element. The decomposition of the carbonates studied in this work follow the expected trend. The least stable carbonate is the $ZnCO_3$, whose decomposition finishes at 325 ° C. The $MgCO_3$ presents an intermediate stability, presenting a decomposition process that culminates at 530 ° C, while the $CaCO_3$ decomposes at temperatures above 750 ° C. The results indicate that carbonate decomposition is effectively achieved.

In order to study the thermal decomposition of the supported carbonates, the corresponding thermogravimetric experiments were carried out. The obtained thermograms are presented in Figure 2. The

theoretical values for loss of CO_2 for each precursor, in the temperature range of 100 °C-750 °C, are presented in Table 3. In this range, the alumina does not present significant changes of mass. Even though the alumina mass loss is small, for the oxidic phases content estimation, the same was subtracted from the mass losses observed for supported catalysts precursors. Experimental and theoretical values for mass loss are quite similar, indicating that the corresponding oxides have been formed. From these results, a composition of 0.27 mol% of each metal can be derived, confirming that three catalysts have the same metal content.

On the other hand, it can be observed that the thermal phenomena occur at lower temperatures for the supported catalysts compared to the bulk ones. It can be predicted that an isothermal treatment of calcination at 600 °C can successfully lead to the formation of supported oxides MgO/γ-Al_2O_3 and ZnO/γ-Al_2O_3. Taking into account the data obtained from the thermal analysis, the calcination temperatures for the different catalysts were determined. The catalysts of magnesium and zinc oxide (bulk and supported) were calcined at 600 °C, the CaO catalyst at 650 °C and the CaO /γ-Al_2O_3 at 750 °C.

Table 4 lists the textural properties of the different catalysts studied, the mg of CO_2 adsorbed per 100 mg of catalyst and the metal oxide crystallite size. As expected, surface area values are higher for supported catalysts than for bulk catalysts. In all the cases, the supported catalysts exhibit lower surface area values than γ-Al_2O_3, but higher pore volume. It is observed that the bulk catalysts have larger pore size values than the supported catalysts. It is possible that these values result from the measurement of interparticular spaces, instead of the intraparticular pores.

The highest value of adsorbed CO_2 is found for MgO/ γ-Al_2O_3 and ZnO/ γ-Al_2O_3 catalysts (Table 4). It can be assumed that a great adsorption corresponds to a higher density of active basic sites for catalysis. Among the prepared supported catalysts, Mg and Zn oxides exhibit the greatest density of basic sites. Nevertheless, the applied technique does not provide information about the strength of those sites.

The isotherms obtained are type IV for bulk and supported oxides (Figures 3-4). Type IV is typical of macro- and mesoporous solids (Thommes *et al.*, 2015). In the isotherm of the bulk catalysts, a hysteresis loop type H3 is observed, while the isotherm of the supported catalysts exhibits hysteresis loop type H2b.

The latter is associated with the blocking or percolation of pores, which would indicate a greater number of surface pores in the supported catalysts.

The XRD obtained patterns, presented in Figure 5, show the presence of the oxide phase in all cases. The X-ray diffraction patterns of CaO and CaO/γ-Al_2O_3 both showed the peaks (JCPDS file No.43-1001) with 2θ at 29.5°, 37.4° and 53.8°, corresponding to CaO phase. For MgO, the diffraction patterns showed the MgO periclase phase, with peaks at 42.7° and 62.2° (JCPDS file No.30-0794). MgO/γ-Al_2O_3 did not present peaks in the pattern. The XRD patterns for ZnO and ZnO/γ-Al_2O_3 showed peaks at 31.8° and 36.3°, corresponding to ZnO phase (JCPDS file No. 36-1451). Comparing the diffraction patterns for the three bulk catalysts, we can notice that the intensity of the peaks corresponding to CaO is smaller than that of the other two. This may be due to a lower crystallinity in the particles thereof. For all samples containing γ-Al_2O_3, the XRD patterns showed wide peaks at 37.0°, 46°and 66° (JCPDS file No. 29-1480) (Umdu *et al.*, 2009). Crystallite sizes are also presented in Table 4. The results show a decrease of size when the oxide is supported. This fact indicates an interaction between metal ions and alumina, according to reported interpretations (Olutoye and Hameed, 2010). The absence of peaks in the MgO/γ-Al_2O_3 pattern indicates that crystallites are too small and dispersed and cannot be measured with the X-ray diffraction technique.

The morphology was analyzed by scanning electron microscopy (SEM). The obtained images are presented in Figure 6. All samples have rough surfaces with a large number of pores. Micrographs are in agreement with the results obtained by N_2 physisorption. Supported oxides show higher surface areas than bulk oxides; moreover, the support can be seen under the agglomerated particles of the metal oxides. In all cases a dispersed phase is formed when the oxide is deposited on alumina, mainly in the case of MgO. Furthermore, the small particles on the catalyst surface have some morphological differences. For example, ZnO/γ-Al_2O_3 has tiny sheets on the surface.

In supported catalysts, the pores can be seen in the micrographs; however, in the case of the bulk ones, it is observed that what the N_2 physisorption technique detects as pores are actually the gaps between the agglomerated particles of the oxides (Limmanee *et al.*, 2013).

3.2 Catalyst activity

3.2.1. Transesterification of soybean oil and castor oil with methanol

As a first screening of the performance of the prepared catalysts, the transesterification reaction using soybean oil and methanol was carried out. The results of conversion at 2, 4 and 6 h are depicted in Figure 7. The conversions reached after 6 h of reaction for bulk Ca, Mg and Zn catalysts were 38%, 13% and 24%, respectively. For supported catalysts, the final conversions were 55%, 60% and 41% for CaO/γ-Al_2O_3, MgO/γ-Al_2O_3 and ZnO/γ-Al_2O_3, respectively. Figure 8 represents the generally accepted mechanism for basic catalyzed transesterification with a metal oxide. First, H^+ is abstracted from basic sites of CH_3OH; methoxide anion is formed. In a second step, the anion attacks the carbon of a carbonyl to generate an alkoxycarbonyl intermediary, which evolves to a more stable fatty acid methyl ester and anion diglyceride. The anion is attracted by a methoxide cation to form a diglyceride. The sequence is repeated twice to finally generate monoglycerides and glycerol (Lam *et al.*, 2010). The increase of catalytic activity is assigned to the electronic properties of the oxides; consequently, basicity increases (Endalew *et al.*, 2011). The presence of alumina improves the dissociation of methanol in CH_3O^- and H^+, which occurs at the superficial basic sites, as can be seen in the first step of the mechanism in Figure 8.

Figure 9 exhibits FAME yield and selectivity to mono- and diglycerides for each catalyst, after 6 h of reaction. MgO/γ-Al_2O_3 presented the highest values of conversion, FAME selectivity and FAME yield, so it can be considered the most active catalyst for the transesterification between soybean oil and methanol. This was the expected result, owing to the high CO_2 adsorption, related to the density of active basic sites, combined with the high surface area value. The reaction occurs superficially; the basic sites are well distributed on the catalyst surface, so the catalyst is more active (di Serio *et al.*, 2006). The low FAME yield reached by CaO/γ-Al_2O_3 (18%) is worth noting. This is due to the leaching of CaO from the catalyst surface, because CaO forms compounds such as calcium diglyceroxide (Gryglewicz, 1999; Pasupulety *et al.*, 2013). It

has been found that the surface of the calcium oxide changes into calcium diglyceroxide after the transesterification reaction. The calcium diglyceroxide in the bulk of the solution acts as the catalyst of the reaction, the OH groups being the active sites (Kouzu *et al.*, 2008). In the same sense, another reason for the low yield reached by the $CaO/\gamma\text{-}Al_2O_3$ catalyst is associated with the lower density of basic sites compared to the other supported catalysts. This was evidenced from the CO_2 adsorption values presented in table 4.

Those catalysts that gave the best results in terms of FAME yield ($MgO/\gamma\text{-}Al_2O_3$ and $ZnO/\gamma\text{-}Al_2O_3$) were submitted to a study to verify that there was no loss of the active phase. To do so, the Mg and Zn contents were determined by atomic absorption spectroscopy on the fresh and used catalysts. As can be seen in Table 5, in both cases the metal concentration remained practically unchanged. This is a very encouraging result, since the leaching of active species is a major problem in the transesterification reaction using heterogeneous catalysts. Since $MgO/\gamma\text{-}Al_2O_3$ and $ZnO/\gamma\text{-}Al_2O_3$ were the most active catalysts in the transesterification of soybean oil and methanol, they were used to continue with the rest of the experiments.

In the transesterification of castor oil with methanol, after 6 h of reaction, conversion values of 39% and 24% for Mg and Zn supported oxides, respectively, were obtained. The conversion result obtained with the $MgO/\gamma\text{-}Al_2O_3$ catalyst is in good agreement with the data published by Negm *et al.* (Negm *et al.,* 2017) who, under similar reaction conditions (castor oil to methanol ratio 1:6, 5 wt% catalyst relative to oil) obtained a 46% conversion but using a rather more sophisticated catalyst than the one used in the present work. On the other hand, the conversion achieved with the $ZnO/\gamma\text{-}Al_2O_3$ catalyst (24%) is also in line with that reported in the literature. (Baskar and Soumiya, 2016).

Figure 10 shows the selectivity for mono-, diglycerides and FAME, and the conversion percentage and FAME yield after 6 h of reaction. FAME yield decreased for both catalysts in comparison with soybean oil (from 57% to 38% for $MgO/\gamma\text{-}Al_2O_3$ and from 31% to 22% for $ZnO/\gamma\text{-}Al_2O_3$). As seen in Table 1, castor oil contains a higher number of free fatty acids than soybean oil, which reduces the catalyst activity by forming soaps in the reaction medium (Barbosa *et al.*, 2010). It is worth emphasizing that FAME selectivity increased considerably for $ZnO/\gamma\text{-}Al_2O_3$ (from 75% to 92% in comparison with soybean oil). This is due to the high

tolerance to free fatty acid that the Zn catalyst has; FAME are generated through triglyceride transesterification and also by esterification of FFA (Yan *et al.*, 2009).

3.2.2. Transesterification of soybean oil and castor oil with butanol

Due to the fact that butanol can be obtained from renewable sources, and the biodiesel generated from this alcohol is completely biodegradable, transesterification was tested using butanol instead of methanol. In the transesterification of soybean oil with butanol, due to the good miscibility between them, the reaction mixture allowed a more efficient contact between the reactants than in the case of methanol (Hájek *et al*., 2016). Conversion values of 50% and 46% for MgO/γ-Al_2O_3 and ZnO/γ-Al_2O_3 catalysts, respectively, were obtained. The conversion values obtained with both catalysts are very good compared with other results found in the literature. Thus, for example, Abreu *et al.* (Abreu *et al.,* 2004) achieved conversions of less than 3% for the transesterification reaction of soybean oil with butanol using metal complexes of Sn, Pb and Zn as acidic catalysts.

The catalysts proved to be completely selective to FABE. The selectivity percentage and FABE yield were practically 100% and 50% for MgO/γ-Al_2O_3, and 97% and 45% for ZnO/γ-Al_2O_3 (Figure 11). Both catalysts were active in the transesterification of soybean oil with butanol. The results were acceptable in comparison with the reaction using methanol, just less active for MgO/γ-Al_2O_3 (57% in FAME yield and 50% in FABE yield) and more active for ZnO/γ-Al_2O_3 (31% in FAME yield and 45% in FABE yield). FABE selectivity increased considerably, almost 100% for both catalysts.

Finally, for the transesterification of castor oil with butanol, the best results were obtained. Conversion values of 97% and 85% were achieved for MgO/γ-Al_2O_3 and ZnO/γ-Al_2O_3, respectively, after 6 h of reaction. FABE selectivity was practically 100% in both cases (Figure 12). The high conversion values can be attributed to the good miscibility between castor oil and butanol. Transesterification occurs in the whole reaction mixture, so the speed of reaction can be favoured (Meneghetti *et al.*, 2007). Besides, the amphoteric properties of ZnO allow the reaction of esterification of FFA present in castor oil to be carried out.

The FABE yield obtained with the MgO/γ-Al_2O_3 catalyst is comparable to those reported in literature by other authors for the transesterification of nonedible oils with *n*-butanol. Thus, for example, Bouaid *et al.* obtained a FABE yield of 96.8% in the transesterification of *rapeseed oil* with butanol using $KOCH_3$ as catalyst (Bouaid *et al.*, 2014) and with the same catalyst, Elboulifi *et al.* achieved a FABE yield of 90% after 8 h of reaction for the transesterification of *jojoba oil* (Elboulifi *et al.,* 2015). On the other hand, Bynes *et al.* achieved a FABE yield of 97.2% in the transesterification of *jatropha oil* catalyzed by H_2SO_4 (Bynes *et* al., 2014). It is worth mentioning that, all these papers are about processes that use homogeneous and/or dangerous solid catalysts in terms of handling. On the contrary, in the present work the use of an innocuous solid is considered, with the advantages that this entails regarding the safety, the minimization of waste and the treatment of residues in the process.

If we compare the values of selectivity to FAAE (fatty acid alkyl ester) reached with the two alcohols used, we can observe that in the butanolysis reactions, for both oils, they were higher regardless of the catalyst used. This can be attributed to the easier abstraction of a proton from butanol compared to methanol, the pKa of butanol is 16.10 while the pKa of methanol is 15.50, which is the first step in the transesterification mechanism (Figure 8) (Wahlen *et al.*, 2008).

The results achieved in this work, obtained with basic catalysis, are promising considering that *castor oil* comes from a nonedible source, and therefore allows the production of second-generation biodiesel. Biodiesel produced from castor oil has high viscosity and an excellent lubricity and can be used in mixtures with fossil diesel or different types of less viscous biodiesel (Meneghetti *et al.*, 2006). Also, butanol can be obtained from a renewable source and the biodiesel produced can be completely biodegradable and has excellent combustion properties.

Conclusions

All the studied catalysts were used in the transesterification of soybean oil with methanol. Especially, the supported ones gave promising results. In particular, MgO/γ-Al_2O_3 gave the best conversion (60%), and

the best results of FAME yield and selectivity (58% and 94% respectively). This can be explained by the modification of electronic properties from the original bulk oxide that causes an increase of the basicity. The catalytic activity was also satisfactory for $ZnO/\gamma\text{-}Al_2O_3$, which gave 41% of conversion, and 31% and 75% of FAME yield and selectivity. Besides, no leaching of the active phase was observed neither for $MgO/\gamma\text{-}Al_2O_3$ nor for $ZnO/\gamma\text{-}Al_2O_3$ catalysts.

Castor oil was evaluated as a source of second-generation biodiesel. When butanol was employed as the alcohol for the transesterification reaction, FABE yields reached values of 97% and 85% for $MgO/\gamma\text{-}Al_2O_3$ and $ZnO/\gamma\text{-}Al_2O_3$ catalysts, respectively. This makes them suitable catalysts for second-generation biodiesel production, taking into account that Castor oil is a nonedible source and butanol is an alcohol that can be obtained from biomass.

Acknowledgements

This work was supported by the Agencia Nacional de Promoción Científica y Tecnológica (Argentina) (PICT-MICINN 2011 N° 2742), the Consejo Nacional de Investigaciones Científicas y Técnicas (CONICET) (PIP N° 0276) and the Universidad Nacional de La Plata (Project X700).

References

Abreu, F.R., Lima, D.G., Hamú, E.H., Wolf, C, Suarez, P.A.Z, 2004. Utilization of metal complexes as catalysts in the transesterification of Brazilian vegetable oils with different alcohols. Journal of Molecular Catalysis A: Chemical 209, 29-33.

Barbosa, D. da C., Serra, T.M., Meneghetti, S.M.P., Meneghetti, M.R., 2010. Biodiesel production by ethanolysis of mixed castor and soybean oils. Fuel 89, 3791–3794.

Baskar, G., Soumiya, S., 2016. Production of biodiesel from castor oil using iron (II) doped zinc oxide nanocatalyst. Renewable Energy 98, 101-107.

Bouaid, A., El boulifi, N., Hahati, K., Martinez, M., Aracil, J., 2014. Biodiesel production from biobutanol. Improvement of cold flow properties. Chemical Engineering Journal 238, 234-241.

Brito, A., Borges, M.E., Garín, M., Hernández, A., 2009. Biodiesel Production from Waste Oil Using Mg–Al Layered Double Hydroxide Catalysts. Energy Fuels 23, 2952–2958.

Bynes, A.N., Eide, I, Jørgensen, K.B., 2014. Optimization of acid catalyzed transesterification of jatropha and rapeseed oil with 1-butanol. Fuel 137, 94-99.

Demirbaş, A., 2003. Biodiesel fuels from vegetable oils via catalytic and non-catalytic supercritical alcohol transesterifications and other methods: a survey. Energy Conversion and Management 44, 2093–2109.

Di Serio, M., Ledda, M., Cozzolino, M., Minutillo, G., Tesser, R., Santacesaria, E., 2006. Transesterification of Soybean Oil to Biodiesel by Using Heterogeneous Basic Catalysts. Ind. Eng. Chem. Res. 45, 3009–3014.

Dias, J.M., Alvim-Ferraz, M.C.M., Almeida, M.F., 2008. Comparison of the performance of different homogeneous alkali catalysts during transesterification of waste and virgin oils and evaluation of biodiesel quality. Fuel 87, 3572–3578.

El-Boulifi, N., Sánchez, M., Martínez, M., Aracil, J., 2015. Fatty acid alkyl esters and monounsaturated alcohols production from jojoba oil using short-chain alcohols for biorefinery concepts. Industrial Crops and Products 69, 244-250.

Endalew, A.K., Kiros, Y., Zanzi, R., 2011. Inorganic heterogeneous catalysts for biodiesel production from vegetable oils. Biomass and Bioenergy 35, 3787–3809.

Georgogianni, K.G., Katsoulidis, A.K., Pomonis, P.J., Manos, G., Kontominas, M.G., 2009. Transesterification of rapeseed oil for the production of biodiesel using homogeneous and heterogeneous catalysis. Fuel Processing Technology 90, 1016–1022.

Gryglewicz, S., 1999. Rapeseed oil methyl esters preparation using heterogeneous catalysts. Bioresource Technology 70, 249–253.

Hájek, M., Skopal, F., Vávra, A., Kocík, J., 2017. Transesterification of rapeseed oil by butanol and separation of butyl ester. Journal of Cleaner Production 155, Part 1 28–33.

Koh, M.Y., Mohd. Ghazi, T.I., 2011. A review of biodiesel production from Jatropha curcas L. oil. Renewable and Sustainable Energy Reviews 15, 2240–2251.

Komers, K., Machek, J., Stloukal, R., 2001. Biodiesel from rapeseed oil, methanol and KOH. 2. Composition of solution of KOH in methanol as reaction partner of oil. Eur. J. Lipid Sci. Technol. 103, 359–362.

Kouzu, M., Kasuno, T., Tajika, M., Yamanaka, S., Hidaka, J., 2008. Active phase of calcium oxide used as solid base catalyst for transesterification of soybean oil with refluxing methanol. Applied Catalysis A: General 334, 357–365.

Lam, M.K., Lee, K.T., Mohamed, A.R., 2010. Homogeneous, heterogeneous and enzymatic catalysis for transesterification of high free fatty acid oil (waste cooking oil) to biodiesel: A review. Biotechnology Advances 28, 500–518.

Lapuerta, M., Armas, O., Rodríguez-Fernández, J. 2008. Effect of biodiesel fuels on diesel engine emissions. Progress in Energy and Combustion Science 34, 198–223.

Lee, H.V., Taufiq-Yap, Y.H., Hussein, M.Z., Yunus, R., 2013. Transesterification of jatropha oil with methanol over Mg–Zn mixed metal oxide catalysts. Energy 49, 12–18.

Limmanee, S., Naree, T., Bunyakiat, K., Ngamcharussrivichai, C., 2013. Mixed oxides of Ca, Mg and Zn as heterogeneous base catalysts for the synthesis of palm kernel oil methyl esters. Chemical Engineering Journal 225, 616–624.

Liu, X., He, H., Wang, Y., Zhu, S., 2007. Transesterification of soybean oil to biodiesel using SrO as a solid base catalyst. Catalysis Communications 8, 1107–1111.

Meneghetti, S.M.P., Meneghetti, M.R., Wolf, C.R., Silva, E.C., Lima, G.E.S., de Lira Silva, L., Serra, T.M., Cauduro, F., de Oliveira, L.G., 2006. Biodiesel from Castor Oil: A Comparison of Ethanolysis versus Methanolysis. Energy Fuels 20, 2262–2265.

Meneghetti, S.M.P., Meneghetti, M.R., Serra, T.M., Barbosa, D.C., Wolf, C.R., 2007. Biodiesel Production from Vegetable Oil Mixtures: Cottonseed, Soybean, and Castor Oils. Energy Fuels 21, 3746–3747.

Nascimento, M.A.R., Lora, E.S., Corrêa, P.S.P., Andrade, R.V., Rendon, M.A., Venturini, O.J., Ramirez, G.A.S., 2008. Biodiesel fuel in diesel micro-turbine engines: Modelling and experimental evaluation. Energy 33, 233–240.

Negm, N.A, Sayed, G.H., Yehia, F.Z., Habib, O.I., Mohamed E.A., 2017. Biodiesel production from one-step heterogeneous catalyzed process of Castor oil and Jatropha oil using novel sulphonated phenyl silane montmorillonite catalyst. Journal of Molecular Liquids 234, 157-163

Ngamcharussrivichai, C., Totarat, P., Bunyakiat, K., 2008. Ca and Zn mixed oxide as a heterogeneous base catalyst for transesterification of palm kernel oil. Applied Catalysis A: General 341, 77-85

Noiroj, K., Intarapong, P., Luengnaruemitchai, A., Jai-In, S., 2009. A comparative study of KOH/Al_2O_3 and KOH/NaY catalysts for biodiesel production via transesterification from palm oil. Renewable Energy 34, 1145–1150.

Olutoye, M.A., M.A. Hameed, M.A., 2010. Transesterification of palm oil on KyMg1−xZn1+xO3 catalyst: Effect of Mg–Zn interaction. Fuel Processing Technology 91, 653–659.

Pasupulety, N., Gunda, K., Liu, Y., Rempel, G.L., Ng, F.T.T., 2013. Production of biodiesel from soybean oil on CaO/Al_2O_3 solid base catalysts. Applied Catalysis A: General 452, 189–202.

Patil, P.D., Gude, V.G., Deng, S., 2009. Biodiesel Production from Jatropha Curcas, Waste Cooking, and Camelina Sativa Oils. Ind. Eng. Chem. Res. 48, 10850–10856.

Patterson, A.L., 1939. The Scherrer Formula for X-Ray Particle Size Determination. Phys. Rev. 56, 978–982.

Prince, R.C., Haitmanek, C., Lee, C.C., 2008. The primary aerobic biodegradation of biodiesel B20. Chemosphere 71, 1446–1451.

Sharma, Y.C., Singh, B., Korstad, J., 2011. Latest developments on application of heterogenous basic catalysts for an efficient and eco friendly synthesis of biodiesel: A review. Fuel 90, 1309–1324.

Steen, E.J., Chan, R., Prasad, N., Myers, S., Petzold, C.J., Redding, A., Ouellet, M., Keasling, J.D., 2008. Metabolic engineering of Saccharomyces cerevisiae for the production of n-butanol. Microb. Cell Fact. 7, 1–8.

Teo, S.H., Taufiq-Yap, Y.H., Ng, F.L., 2014. Alumina supported/unsupported mixed oxides of Ca and Mg as heterogeneous catalysts for transesterification of Nannochloropsis sp. microalga's oil. Energy Conversion and Management 88, 1193–1199.

Thommes, M., Kaneko, K., Neimark, A.V., Olivier, J.P., Rodriguez-Reinoso, F., Rouquerol, J., Sing, K.S.W., 2015. Physisorption of gases, with special reference to the evaluation of surface area and pore size distribution (IUPAC Technical Report). Pure and Applied Chemistry 87, 1051–1069.

Ullah, F., Dong, L., Bano, A., Peng, Q., Huang, J., 2016. Current advances in catalysis toward sustainable biodiesel production. Journal of the Energy Institute 89, 282–292.

Umdu, E.S., Tuncer, M., Seker, E., 2009. Transesterification of Nannochloropsis oculata microalga's lipid to biodiesel on Al_2O_3 supported CaO and MgO catalysts. Bioresource Technology 100, 2828–2831.

Wahlen, B.D., Barney, B.M., Seefeldt, L.C., 2008. Synthesis of Biodiesel from Mixed Feedstocks and Longer Chain Alcohols Using an Acid-Catalyzed Method. Energy Fuels 22, 4223–4228.

Wan, T., Yu, P., Gong, S., Li, Q., Luo, Y., 2008. Application of KF/MgO as a heterogeneous catalyst in the production of biodiesel from rapeseed oil. Korean J. Chem. Eng. 25, 998–1003.

Williamson, G.K., Hall, W.H., 1953. X-ray line broadening from filed aluminium and wolfram. Acta Metallurgica 1, 22–31.

Yan, S., Salley, S.O., K.Y. Simon Ng, K.Y., 2009. Simultaneous transesterification and esterification of unrefined or waste oils over ZnO-La2O3 catalysts. Applied Catalysis A: General 353, 203–212.

Zhang, Z., Wang, B., Sun, Q., Zheng, L., 2014. A novel method for the preparation of CO_2 sorption sorbents with high performance. Applied Energy 123, 179–184

Zheng, Y., Chen, X., Shen, Y. 2008. Commodity Chemicals Derived from Glycerol, an Important Biorefinery Feedstock. Chem. Rev. 108, 5253-5277.

Table 1. Fatty acid composition (%) of soybean oil and castor oil (Meneghetti *et al*. 2007, 2006)

Fatty acid	Fatty acid content (%)	
	Soybean oil	Castor oil
Myristic (14:0)	0.2	-
Palmitic (16:0)	16.0	1.8
Stearic (18:0)	2.4	-
Oleic (18:1)	23.5	-
Linoleic (18:2)	51.2	11.2
Linolenic (18:3)	8.5	-
Ricinoleic (18:0(OH))	-	87.0
Total C18	85.6	98.2
Free fatty acids (FFA)	0.1	1.2

Table 2. Theoretical and experimental values for weight loss for mass precursors.

Sample	% Theoretical weight loss	% Experimental weight loss
$CaCO_3$	43.96	44.47
$MgCO_3$	52.18	65.54
$ZnCO_3$	35.09	31.97

Table 3. Theoretical and experimental values of weight loss for supported precursors.

Sample	% Theoretical supported oxide	% Theoretical weight loss	% Experimental weight loss
$CaCO_3/\gamma\text{-}Al_2O_3$	13.53	10.61	9.70
$MgCO_3/\gamma\text{-}Al_2O_3$	9.73	10.61	9.45
$ZnCO_3/\gamma\text{-}Al_2O_3$	19.64	10.61	10.24

Table 4. Physicochemical characteristics of the catalysts

Catalyst	S_{BET} (cm^2/g)	V_{pore} (cm^3/g)	d_{pore} (Å)	%mg CO_2ads	$d_{cristallyte}$ (nm)
CaO	15	0.12	309	-	24
MgO	14	0.04	119	-	24
ZnO	7	0.02	119	-	32
CaO/γ-Al_2O_3	141	0.37	106	0.180	14
MgO/γ-Al_2O_3	223	0.43	77	0.258	-
ZnO/γ-Al_2O_3	173	0.42	98	0.259	18
γ-Al_2O_3	252	0.36	58	-	-

Table 5. Wt% of MgO and ZnO on γ-Al_2O_3 after and before the transesterification between soybean oil and methanol

Catalyst	Wt% after reaction	Wt% beforereaction
MgO/γ-Al_2O_3	8	8
ZnO/γ-Al_2O_3	11	11

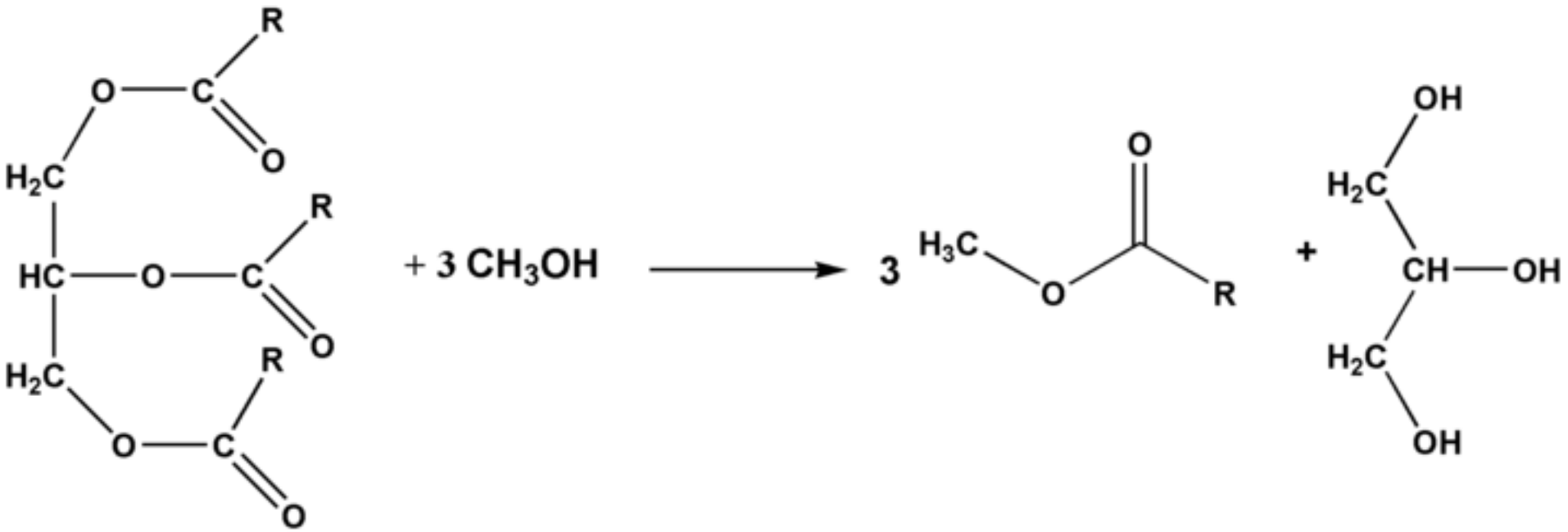

$$MCO_3\,(s) \rightleftharpoons MO\ (s) + CO_2\,(g) \qquad \text{Scheme 2}$$

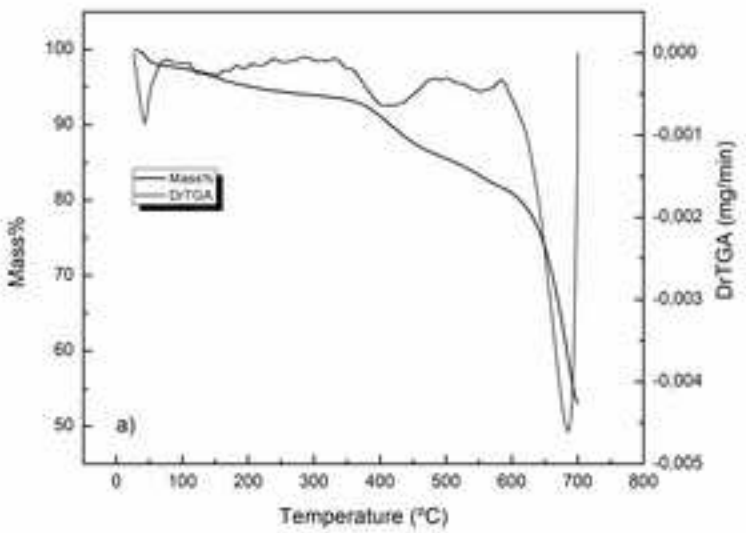

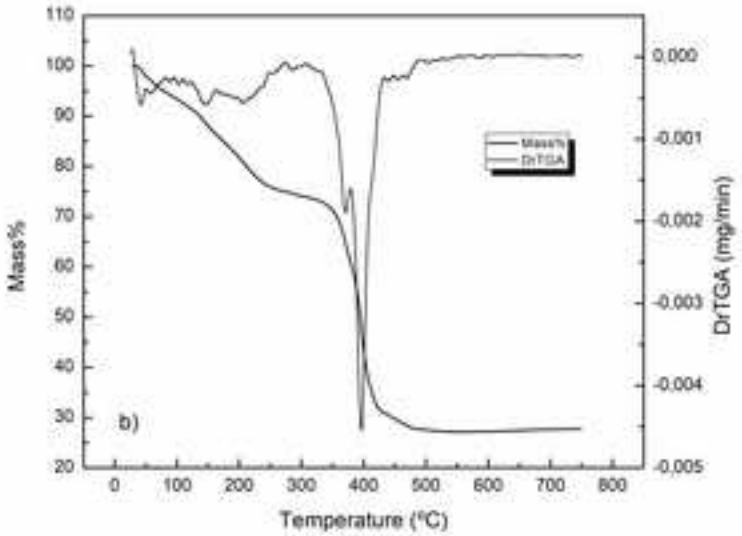

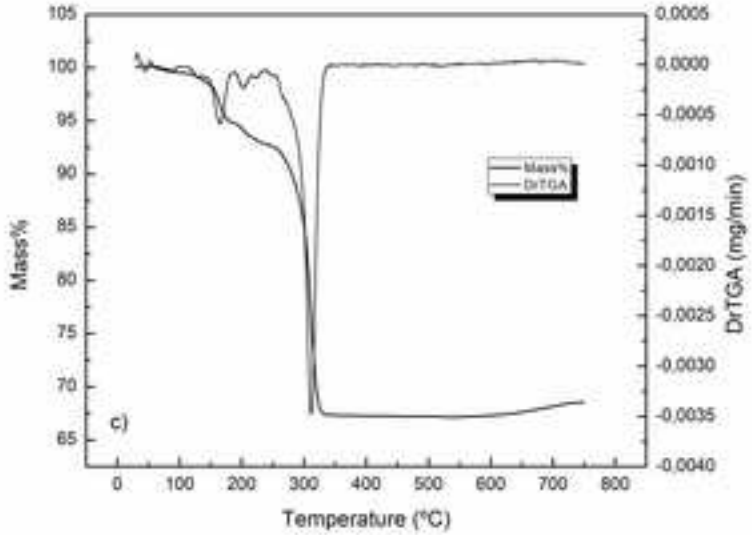

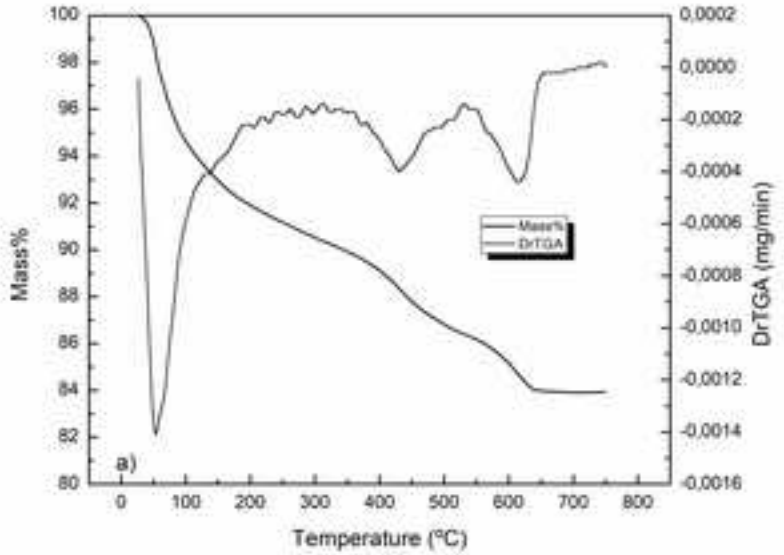

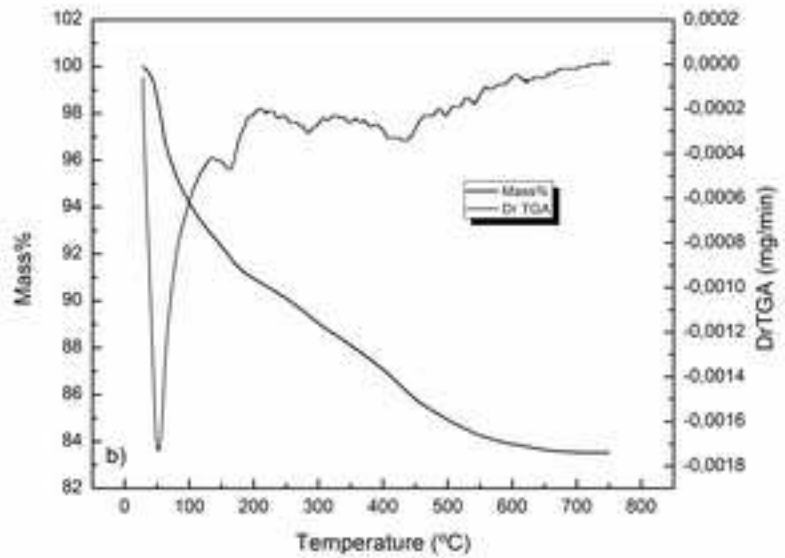

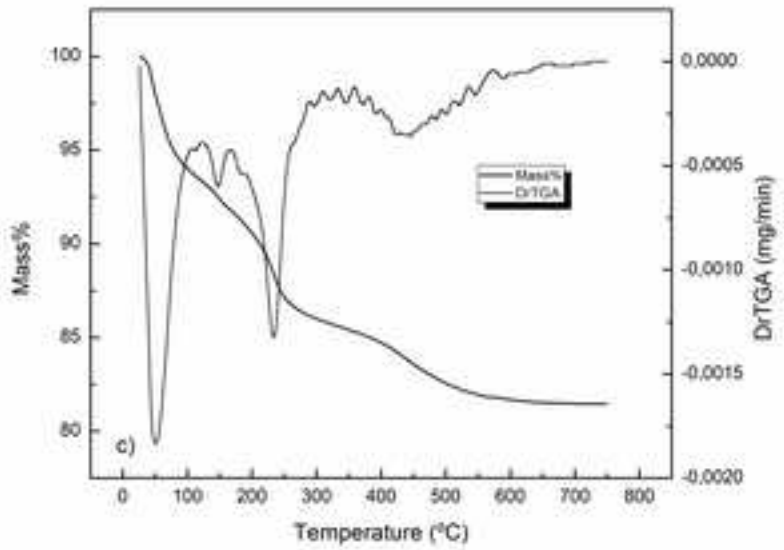

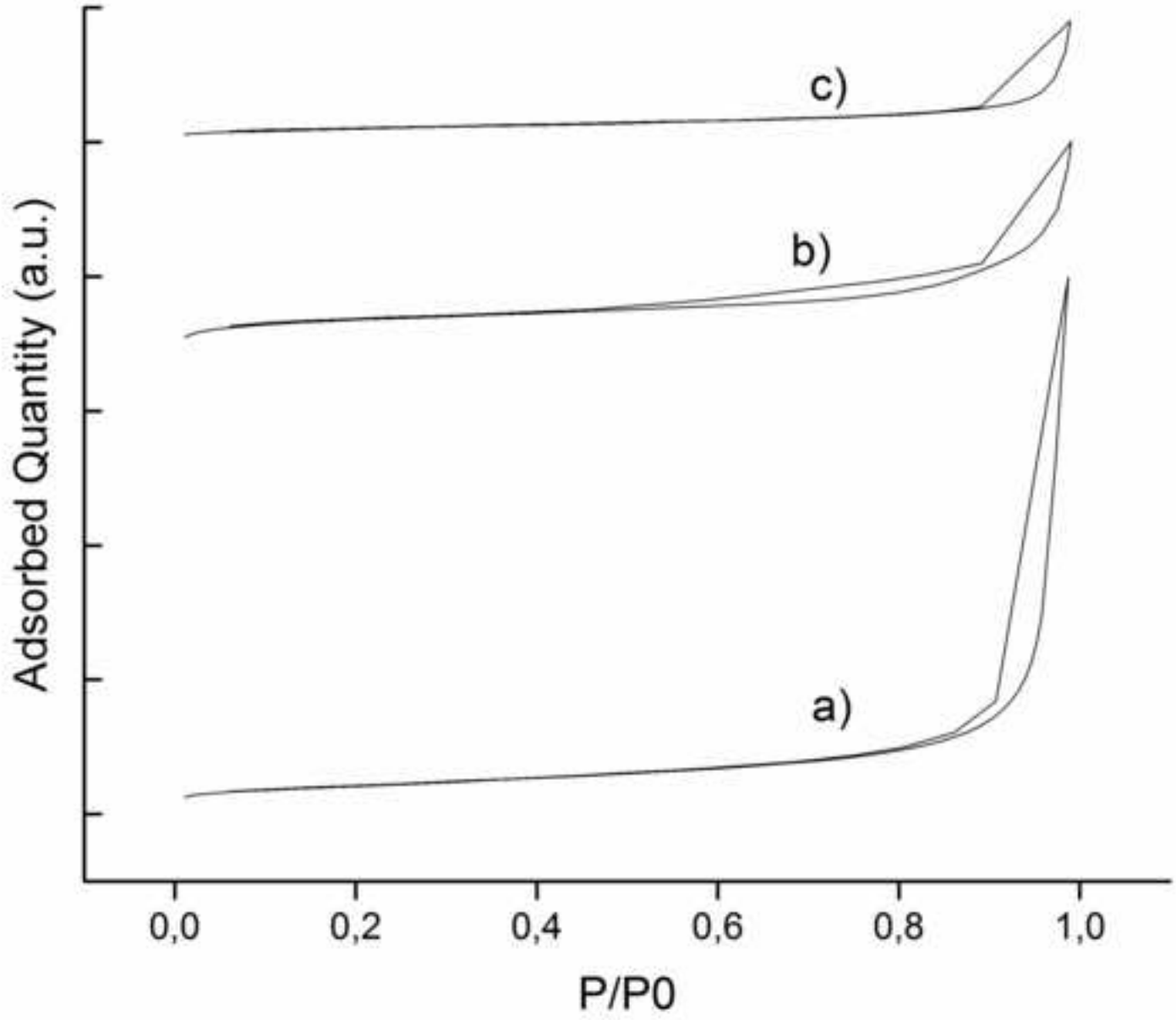

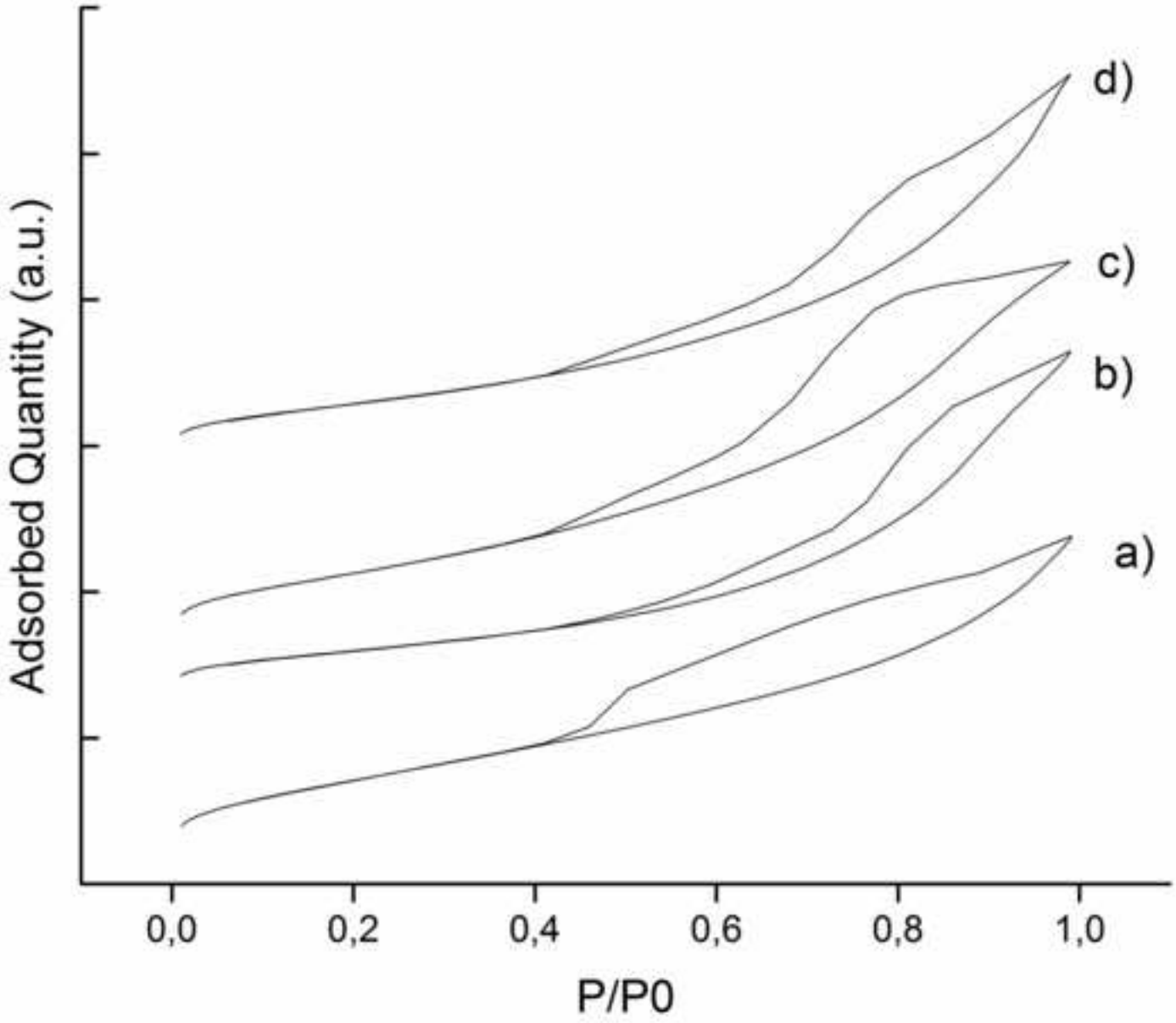

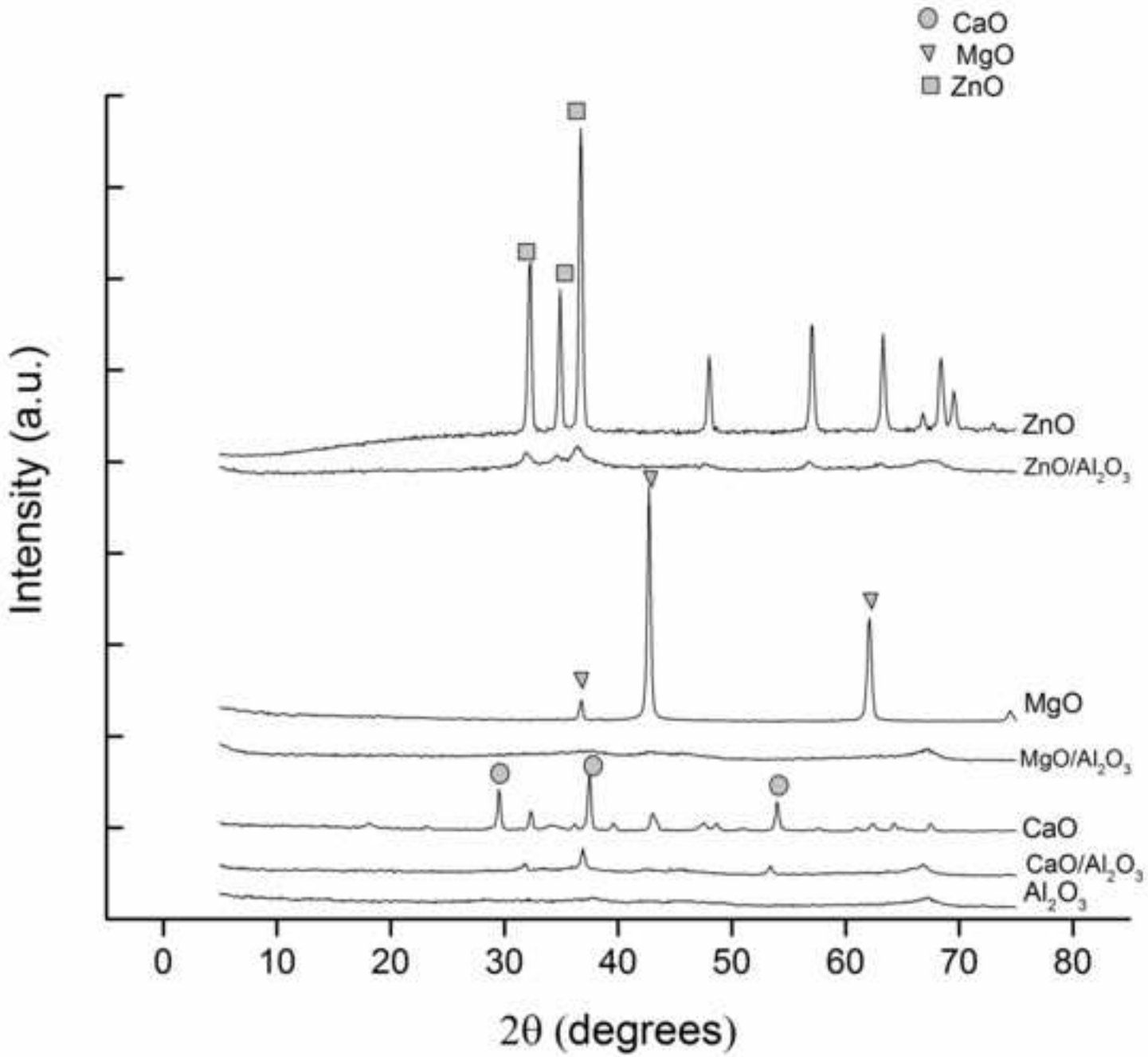

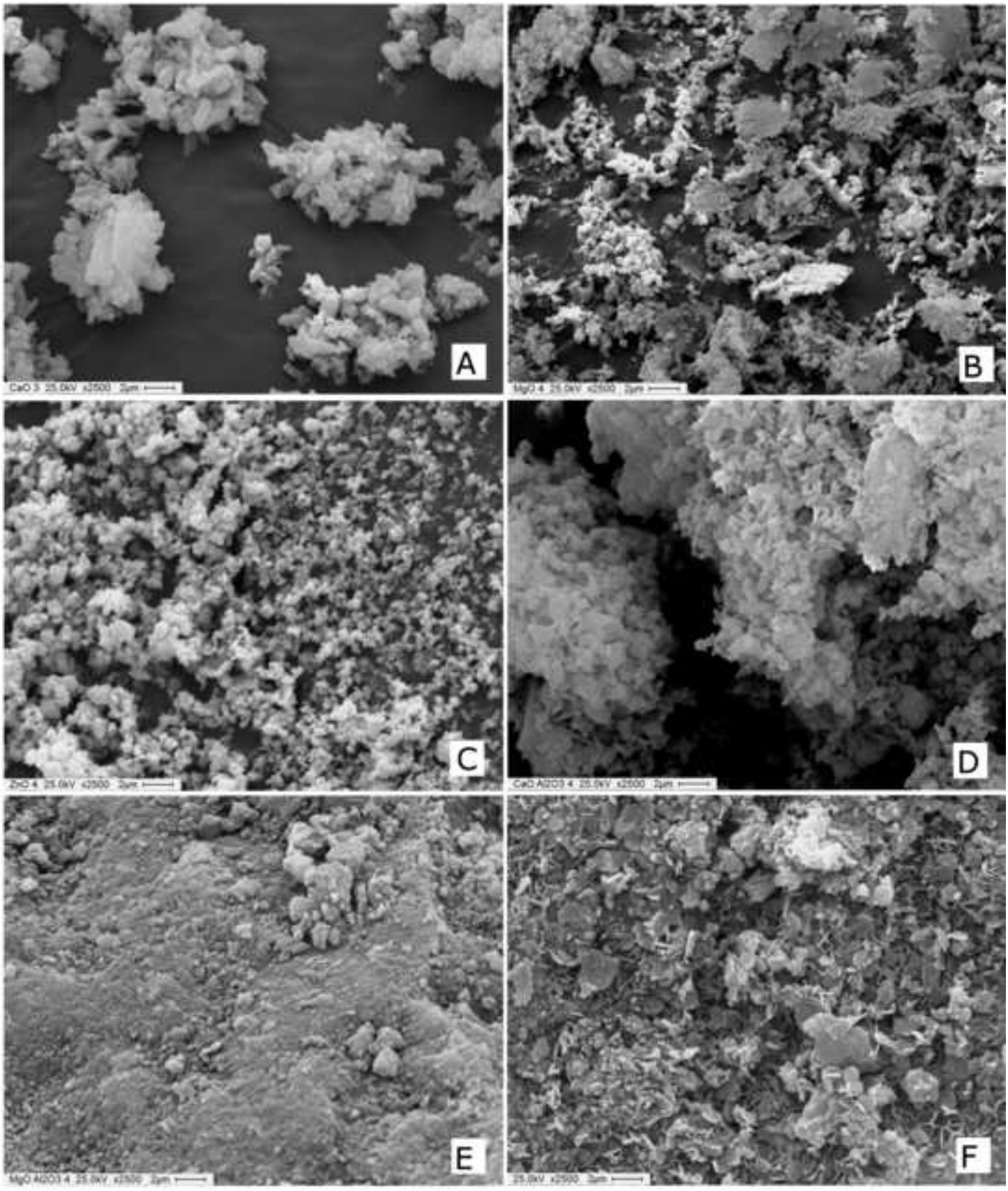

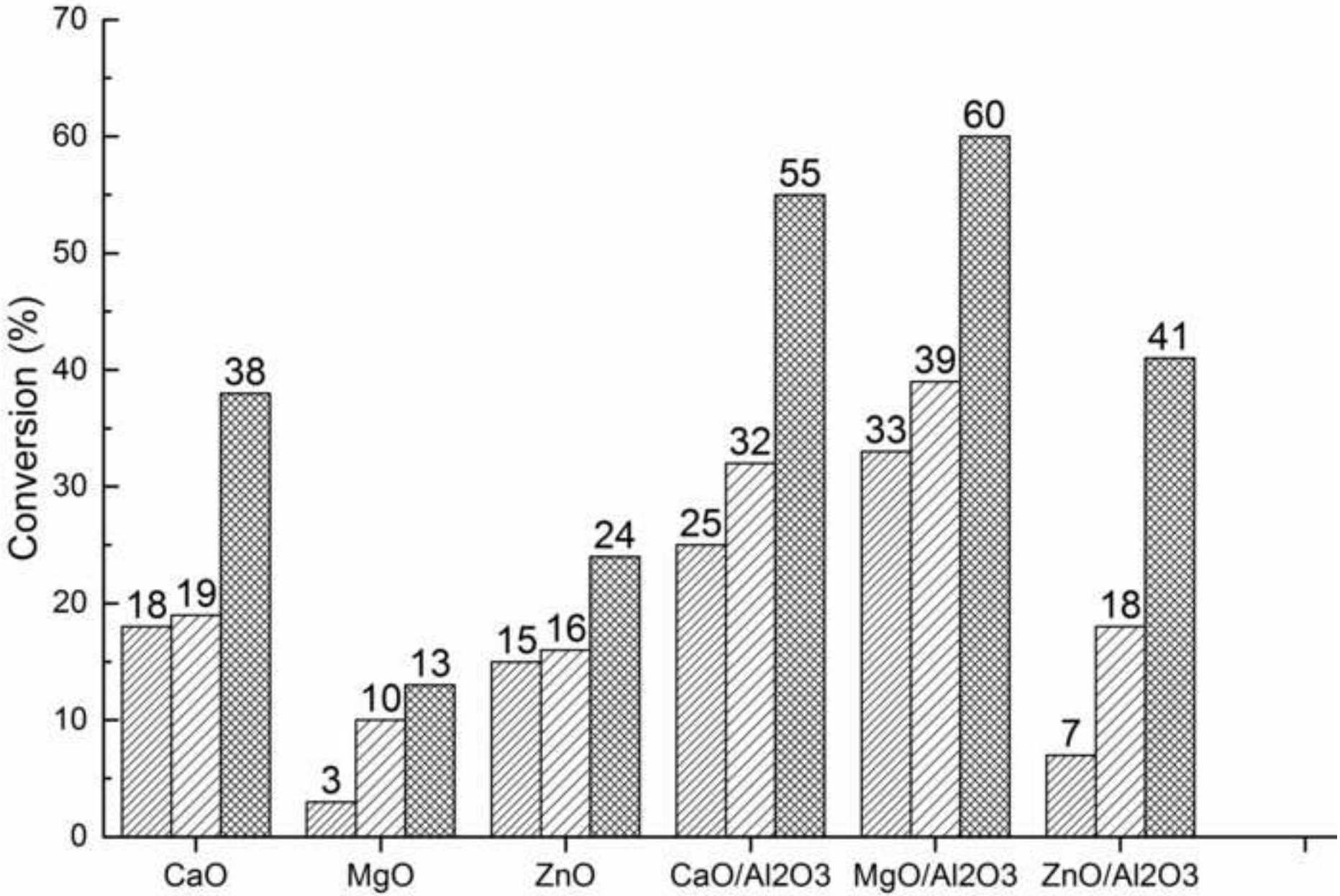

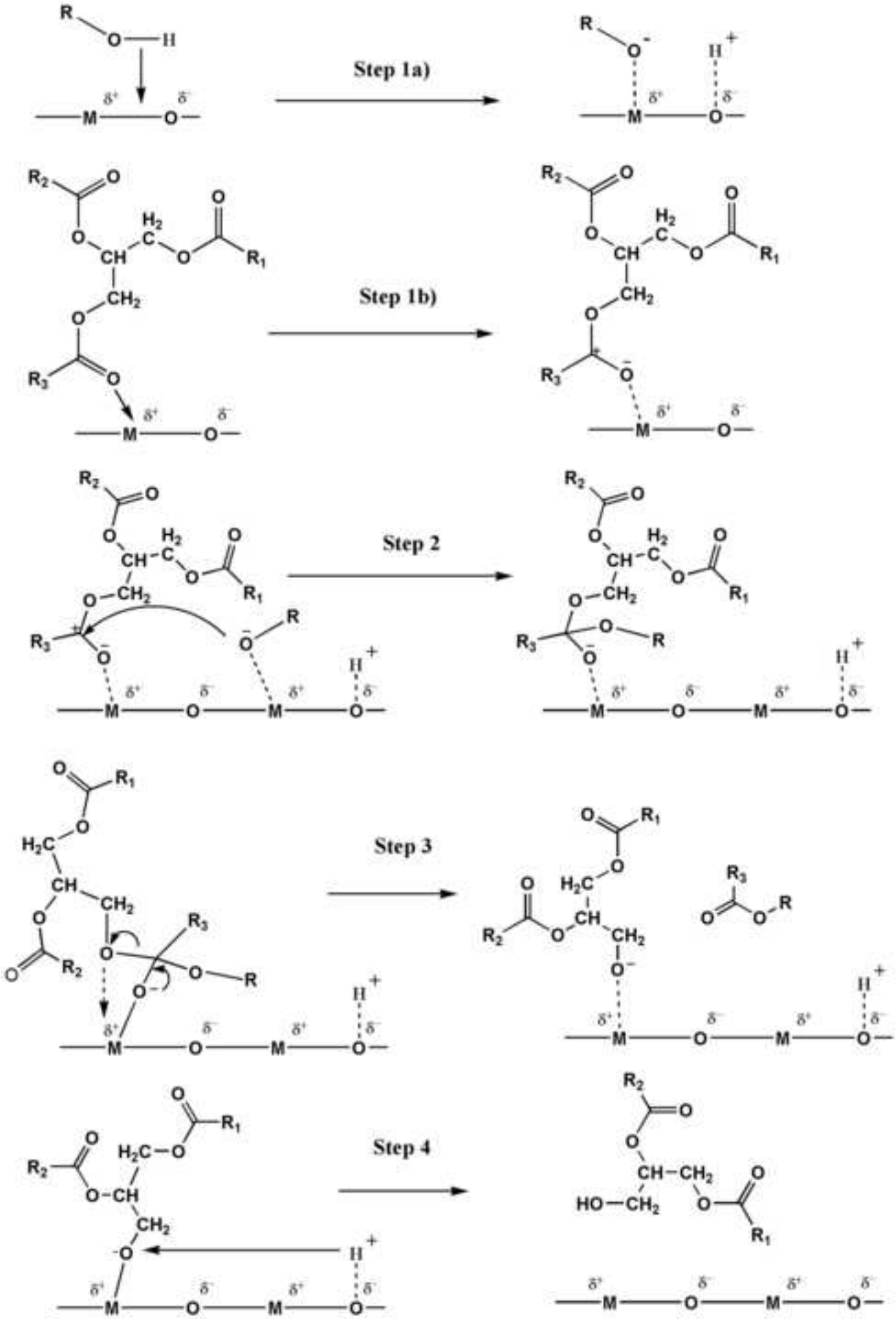

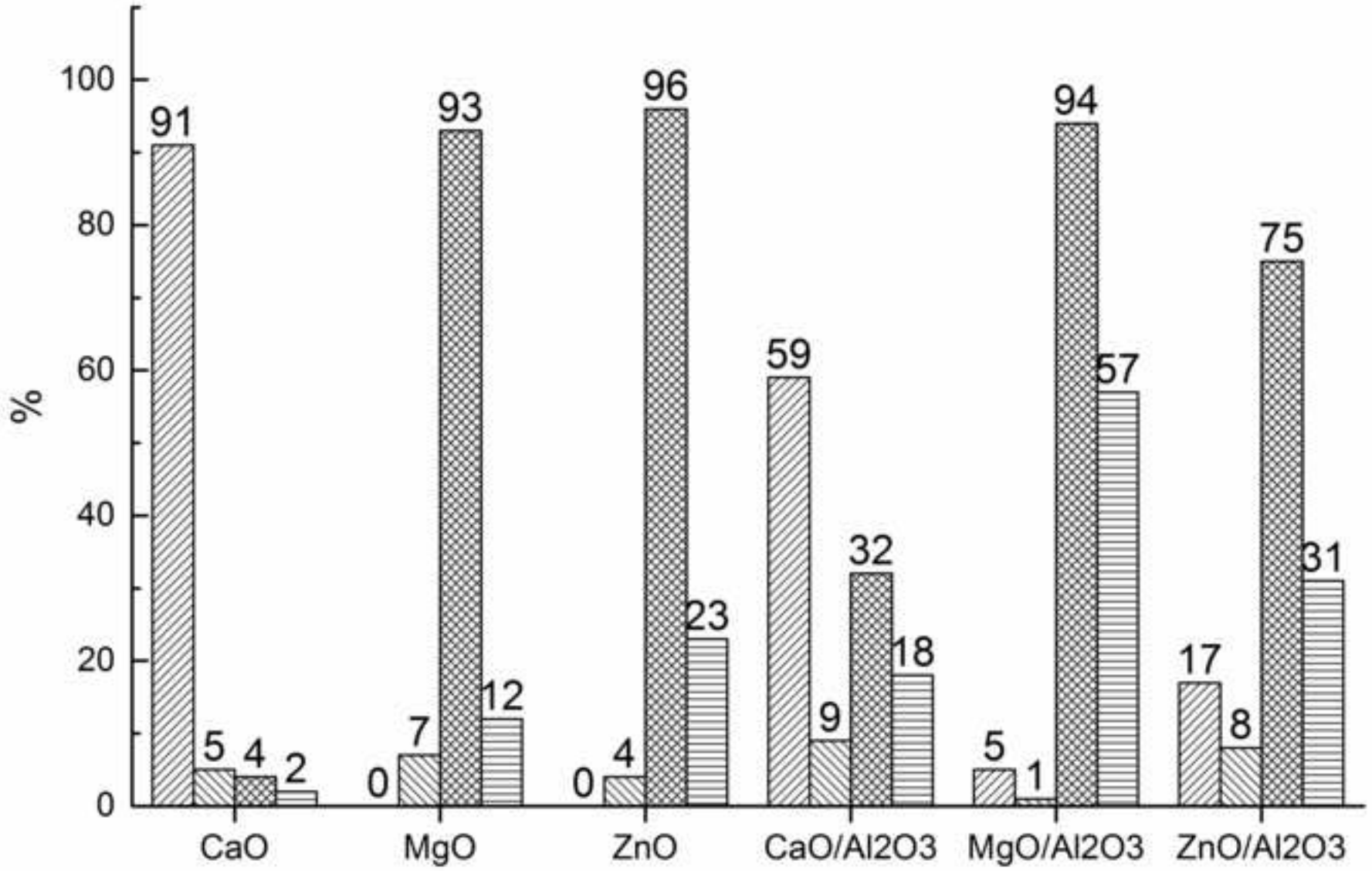

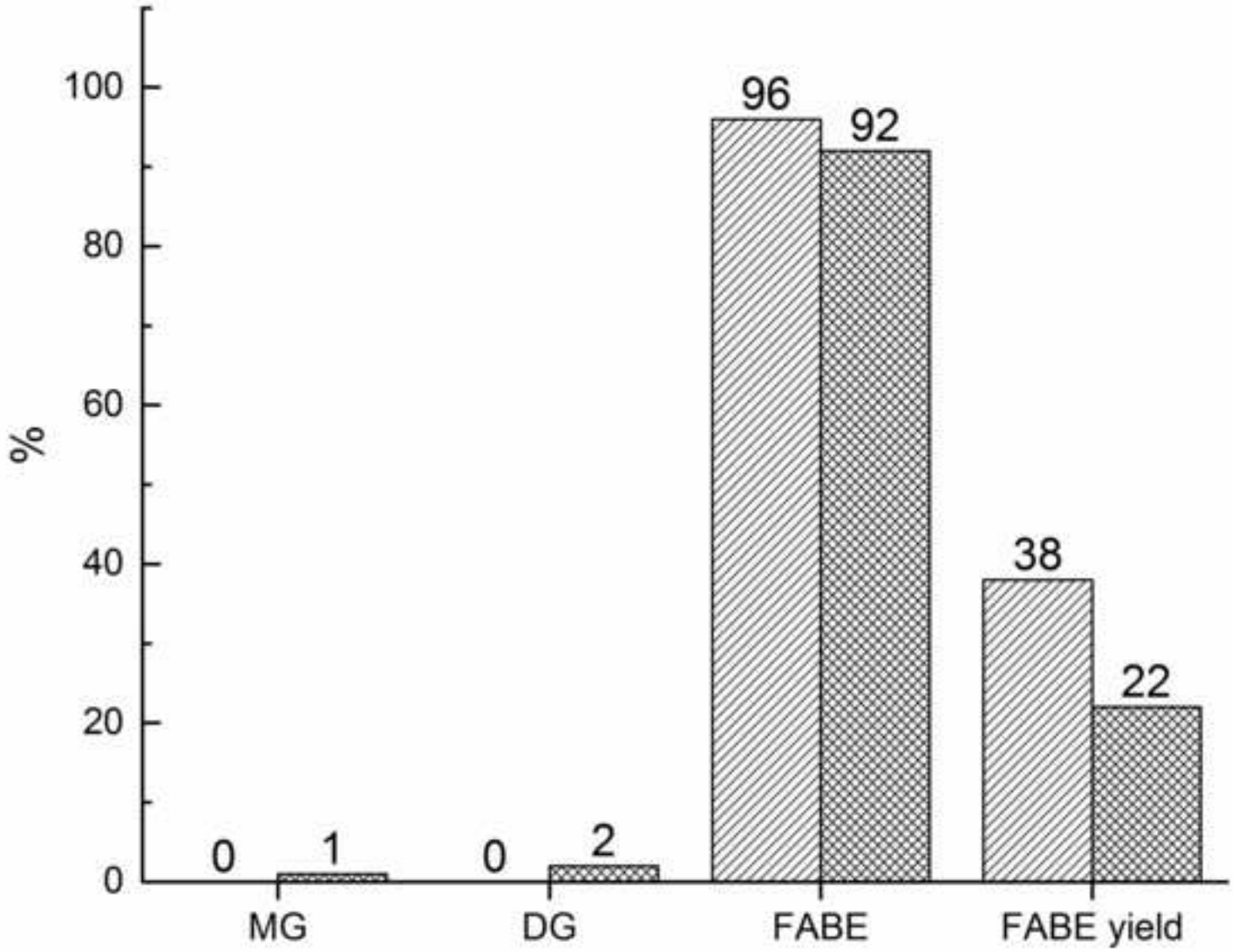

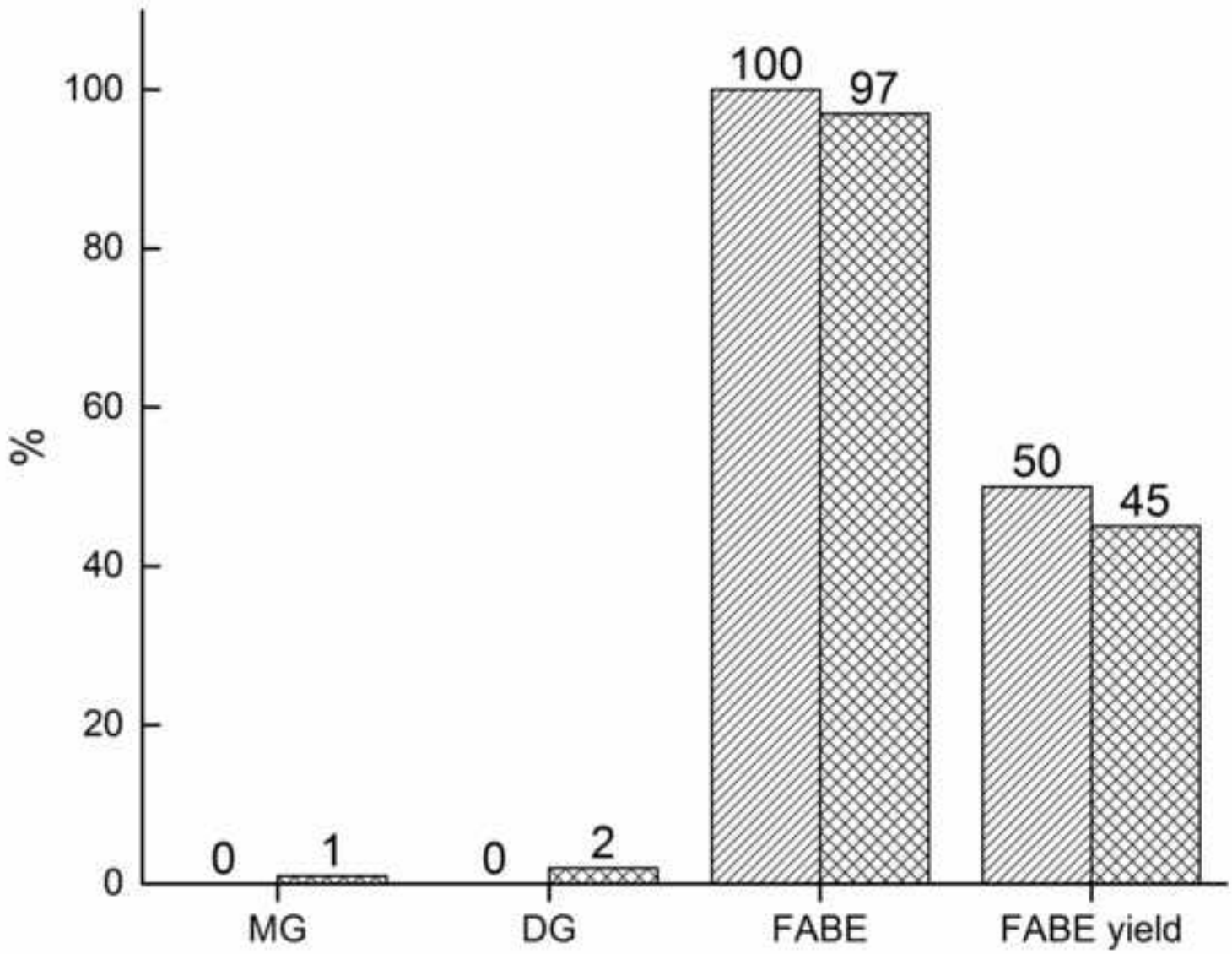

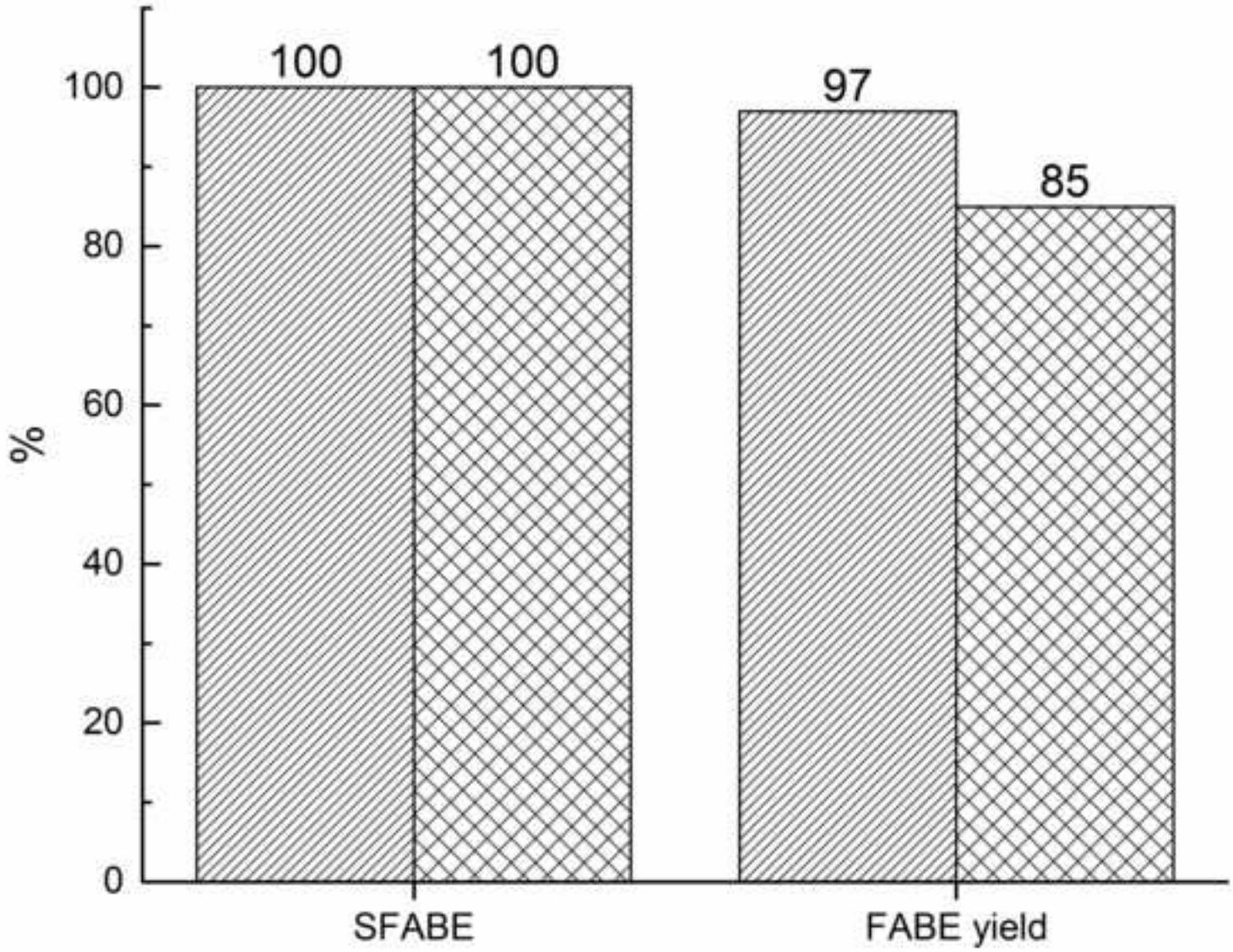

Figure 1. Thermograms obtained for mass catalysts. a) CaO, b) MgO, c) ZnO

Figure 2. Thermograms obtained for supported catalysts. A) CaO/γ-Al_2O_3 B) MgO/γ-Al_2O_3 C) ZnO/γ-Al_2O_3

Figure 3. BET isotherms for mass catalysts. a) CaO; b) MgO and c) ZnO

Figure 4. BET isotherms for supported catalysts. A: γ-Al_2O_3; B: CaO/γ-Al_2O_3; C: MgO/γ-Al_2O_3 and D: ZnO/γ-Al_2O_3

Figure 5. XRD patterns of different catalysts

Figure 6. SEM images for each catalyst, at 2500X. A: CaO; B: MgO; C: ZnO; D: CaO/γ-Al_2O_3; E: MgO/γ-Al_2O_3; F: ZnO/γ-Al_2O_3

Figure 7. Conversion percentage vs. time for different catalyst in the transesterification of soybean oil and methanol, at 2h(▨), 4h(◪), and 6h(▩)

Figure 8. General mechanism for transesterification reaction with a basic heterogeneous catalyst

Figure 9. Selectivity percentage to monoglycerides(▨) diglycerides (▧) and FAME (▩), and FAME yield (▤), for each catalyst in the transesterification of soybean oil and metanol, elapsed 6 h.

Figure 10. Selectivity to monoglycerides (MG), diglycerides (DG) and FAME; and FAME yield for Mg (▨) and Zn (▩) supported oxides, after 6h in the transesterification between castor oil and methanol.

Figure 11. Selectivity to monoglycerides (MG), diglycerides (DG) and FABE; and FABE yield, of MgO (▨) and ZnO (▩) supported catalysts after 6h of reaction, in the transesterification between soybean oil and butanol.

Figure 12. Selectivity to FABE (SFABE) and FABE yield for transesterification of castor oil with butanol for Mg (▨) and Zn (▩) supported catalysts

Highlights

- Transesterification reaction of soybean and castor oil using solid base catalyst
- Higher selectivity to fatty acid esters when butanol was used instead of methanol
- MgO/γ-Al_2O_3 catalyst showed more than 97% to FABE yield with castor oil
- More than 85% of FABE yield was achieved with ZnO/γ-Al_2O_3 and castor oil